Passenger vehicle behavior modeled by Power Flow using different mathematical tire models

Ricardo T. C. Neto[1], Bruna R. Loiola[1]

[1]*Dept. of Mechanical Engineering, Military Institute of Engineering*
Praça Gen. Tibúrcio, 80, 22290-270, Rio de Janeiro/RJ, Brazil
ricardo@ime.eb.br, bruna.loiola@ime.eb.br

Abstract. Ground Vehicles can be approached as a set of integrated subsystems, with cause-effect relationships. Through the Power Flow Modeling approach, each of these subsystems can be interpreted as a black box, and interrelated with the others in a modular way, as long as causalities are respected. This work aims to take advantage of the modularity of the automobile interpreted as a set of integrated subsystems and evaluate the influence of mathematical tire models on its acceleration and braking behavior. Each of the subsystems is mathematically modeled in individual blocks that are then integrated, without loss of causality, in MATLAB/Simulink® software. The purpose is to provide a fully modular vehicle model, taking advantage of this Power Flow feature, in an open-source code. Furthermore, Inverse Problems are applied to estimate parameter values of the Burckhardt mathematical model in order to obtain similar behaviors of the corresponding tire model by the Magic Formula.

Keywords: Power Flow, Longitudinal Vehicle Dynamics, Brake Performance, Tire Mathematical.

1 Introduction

The performance of a land vehicle when accelerating and/or braking depends heavily on the behavior of the tires. There are several mathematical models developed to represent tires [1]. The one that stands out most is the Magic Formula, introduced by Bakker, Pacejka, and Lidner [2]. However, land vehicles can be approached as a set of integrated systems, which facilitates the analysis and understanding of how each of these interacts with the others. Each of these systems has its cause-and-effect relationships, which, if well understood, allow them to be approached as a module. Thus, observing the architecture of each of the systems, it is possible to separate their relevant elements into integrated modules that can even be replaced by others that fulfill the same functions, as long as their respective causalities are respected. The blocks' interaction takes place through Power Flow, where only power variables, efforts, and speeds are passed from one block to another, as proposed in the thesis of Costa Neto [3], a methodology characterized by modularity. This allows the vehicle to be represented in a block diagram, and the mathematical model to be written in Simulink in MATLAB® environment.

In this context, the objective of this work is to present a modular mathematical model of a two-axle land vehicle, in which the powertrain and the braking system are represented in block diagrams. Each element of these subsystems is incorporated into the block where it is physically mounted in a passenger vehicle. The architecture is such that the main structure is maintained, while the blocks representing the tires are easily replaced by others without resulting in significant changes. It is also possible to vary the traction, choosing between front-wheel drive, rear-wheel drive, or all-wheel drive (4 x 4).

2 Mathematical Formulation

The passenger vehicle is modeled following the ISO 8855 [5] reference in Cartesian Coordinates, originating at its center of mass, as shown in Fig. 1a. The plan model (xz plane) has three degrees of freedom – vehicle displacement in the direction x and rotation of each wheel around its spin axis (Double Corner Vehicle Model). The stiffness and damping effects of the suspensions are not considered. The free-body diagram to obtain the equations of motion is represented in Figures 1a and 1b.

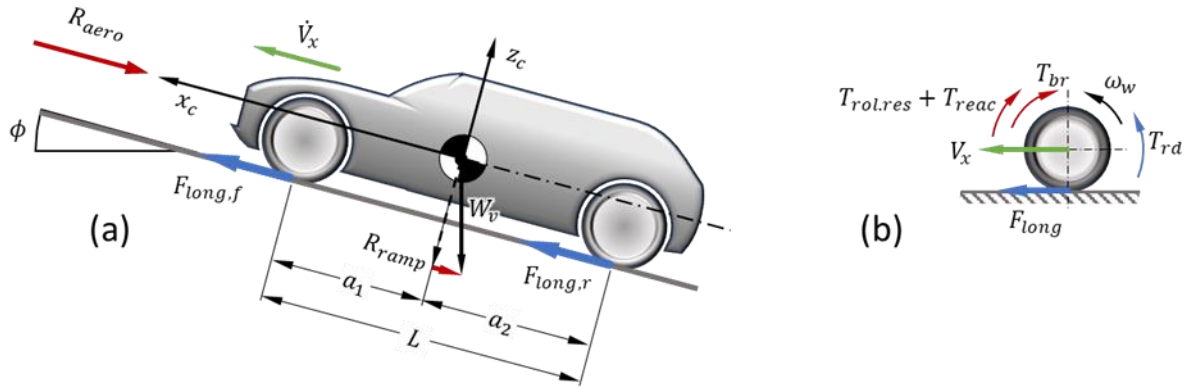

Figure 1. (a) Free body diagrams of a whole vehicle; (b) free body diagram of a wheel; front and rear wheels have the same FBD (source: authors).

Where:
a_1 and a_2 – distances from the front and rear wheels center to the vehicle center of gravity;
L – vehicle wheelbase;
$F_{long,f}$ and $F_{long,r}$ – front and rear tires longitudinal forces;
R_{Aero} – aerodynamic drag force;
$T_{rol,res}$ – tire rolling resistance torque from its rolling movement;
T_{reac} – tire reaction torque from its longitudinal tire force;
T_{br} – brake torque from the vehicle brake system;
T_{rd} – traction torque from the vehicle transmission system;
V_x – vehicle and wheel centers longitudinal velocity;
ω_w – wheel angular velocity;
ϕ – ramp angle.

2.1 Powertrain system

The Powertrain system is responsible for moving the vehicle, including everything from the engine to the driving wheels (Fig. 2). Each of the blocks contains an expression that represents the functioning of the mechanical system, and each WHEEL + TIRE block also contains the Euler equation of motion for that set. Tab. 1 presents the relevant expressions (this block is the same used in both subsystems, Powertrain and Brake).

In all blocks listed, the input variables are speeds, and the output variables are efforts. The DRIVER and SELECTOR T-TYPE blocks participate indirectly in the system dynamics. In the T-TYPE SELECTOR block, the user chooses the type of traction: 1 for front-wheel drive, 2 for rear-wheel drive, and 3 for all-wheel drive. The DRIVER block contains the function for changing gears, which is done according to the vehicle's speed.

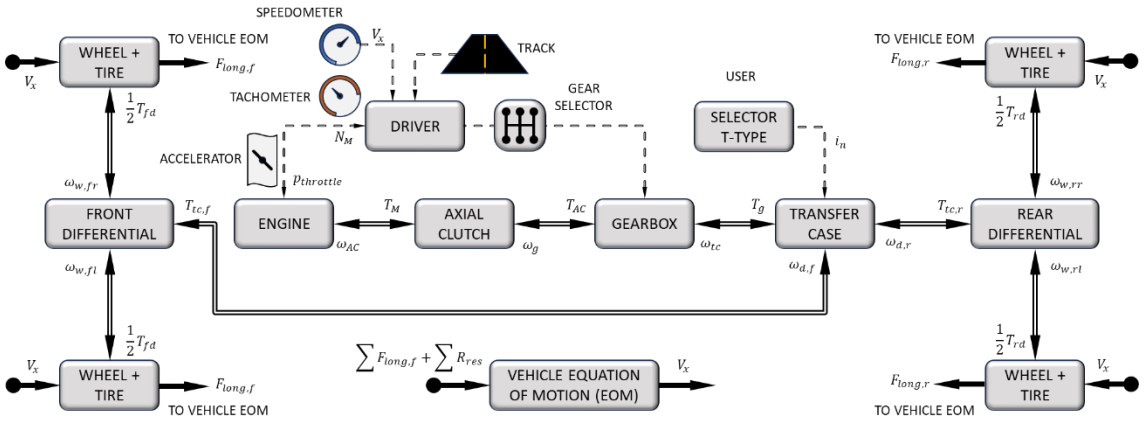

Figure 2. Powertrain block diagram (source: authors)

Table 1. Expressions relevant to each block in the powertrain diagram

Block	Expression	Eq
ENGINE [5]	$T_M(\omega_{AC}) = (p_{throttle})(P_1 + P_2\omega_{AC} + P_3\omega_{AC}^2)$	(1)
AXIAL CLUTCH	$T_{AC} = \eta_{AC} T_M$	(2a)
	$\omega_{AC} = \omega_g$	(2b)
GEARBOX [5]	$T_g = (\eta_g i_n) T_{AC}$	(3a)
	$\omega_g = i_n \omega_{tc}$	(3b)
TRANSFER CASE	$\text{T}-\text{TYPE} = 1 \implies \begin{cases} T_{tc,f} = (\eta_{tc} i_{tc}) T_g, & T_{tc,r} = 0 \\ \omega_{tc} = i_d \omega_{d,f} \end{cases}$	(4a) (4b)
	$\text{T}-\text{TYPE} = 2 \implies \begin{cases} T_{tc,r} = (\eta_{tc} i_{tc}) T_g, & T_{tc,f} = 0 \\ \omega_{tc} = i_d \omega_{d,r} \end{cases}$	(4c) (4d)
	$\text{T}-\text{TYPE} = 3 \implies \begin{cases} T_{tc,f} = (1/2)\,(\eta_{tc} i_{tc}) T_g \\ T_{tc,r} = (1/2)\,(\eta_{tc} i_{tc}) T_g \\ \omega_{tc} = (1/2) i_{tc} (\omega_{d,f} + \omega_{d,r}) \end{cases}$	(4e) (4f) (4g)
DIFFERENTIAL (FRONT and REAR)	$T_{rd,j} = (1/2)(\eta_d i_d) T_{tc}$	(5a)
	$\omega_{d,j} = i_d (1/2)(\omega_{w,r,j} + \omega_{w,l,j})$	(5b)
WHEEL + TIRE j(*)	$\omega_{w,j} = \int_{t=0}^{t=\tau} (T_{rd,j} - T_{b,j} - T_{rol.res\,,j} - r_{din} F_{long,j}/I_{yy}) dt$	(6)
	$F_{long,j} = f(F_{Z,j}, i_{x,j})$	(7)
	$i_{x,j} = (\omega_{w,j}\, r_{est} - V_x)/V_x$	(8)

(*) Torques $T_{rd,j}$ e $T_{b,j}$ are not applied simultaneously.

In this work, the engine is modeled operating in a steady state, and the torque it produces, T_M, is represented by a second-degree polynomial (eq. 1) in which the constants P_1, P_2, and P_3 are calculated from the maximum power and corresponding engine angular speed [5]. The ENGINE block input variable is the angular velocity from the AXIAL CLUTCH, ω_{AC}. The engine torque is then delivered to the AXIAL CLUTCH block, responsible for coupling the movement between the engine and the GEARBOX, which transmits it with losses, represented by the efficiency η_{AC} (eq. 2a). In the AXIAL CLUTCH block the input and output speeds are equal (eq. 2b). In the GEARBOX, the torque from AXIAL CLUTCH is multiplied by the transmission ratio of the n-th gear, which is selected in the DRIVER block, i_n, and is transmitted with losses represented by the efficiency η_g (eq. 3a). The speed coming from the TRANSFER CASE block, ω_{tc}, is multiplied by the same i_n, (eq. 3b). Gear selection depends on the vehicle speed, established by the gearbox Speed Diagram [5]. The output torque T_g is then transferred to the TRANSFER CASE block, where one can select one of three traction options, FWD, RWD, or AWD. The open differential transmission ratio is i_{tc}, and its efficiency is η_{tc}. The eq. 4a to 4g shows the rules that define the torque

distribution to the axles. The TRANSFER CASE output torque is multiplied by the axle differential gear ratio, i_d, with losses, η_d (eq. 5a). The FRONT/REAR DIFFERENTIAL blocks (both open differentials) receive the angular speeds of each wheel, right and left side, and deliver the half sum of these speeds (eq. 5b). The angular velocity of each wheel, whose FBD is represented in Fig. 1b, is calculated by Euler's equation (eq. 6) in the WHEEL+TIRE block, where I_{yy} is the moment of inertia of rotation around its spin axis. The WHEEL+TYRE block also contains the tire model (eq. 7) and the tire longitudinal slip (eq. 8) equations. Finally, the calculated angular velocity $\omega_{w,j}$ is the FRONT/REAR DIFFERENTIAL block input variable. Then, in the powertrain system, the "dynamic path" is – eq. 1 → eq. 2a → eq. 3a → eq. 4a (or 4c, or 4e/4f) → eq. 5a → eq. 6/7/8 – and the "kinematic path" – eq. 6 → eq. 5b → eq. 4b (or 4d, or 4g) → eq. 3b → eq. 2b → eq. 1. The DRIVER block acts like a "controller block", using the engine angular velocity, N_M (TACHOMETER), and the vehicle velocity, V_x (SPEEDOMETER). Longitudinal forces are passed to the VEHICLE EQUATION OF MOTION (EOM) block, with the sum of the resistances. The output variable is the vehicle velocity, V_x.

2.2 Hydraulic brake system

In the hydraulic brake system, power only flows in one direction; there is no speed response linked directly to the effort delivered as presented in Fig. 3. The system's equations shown below are found in Limpert [6].

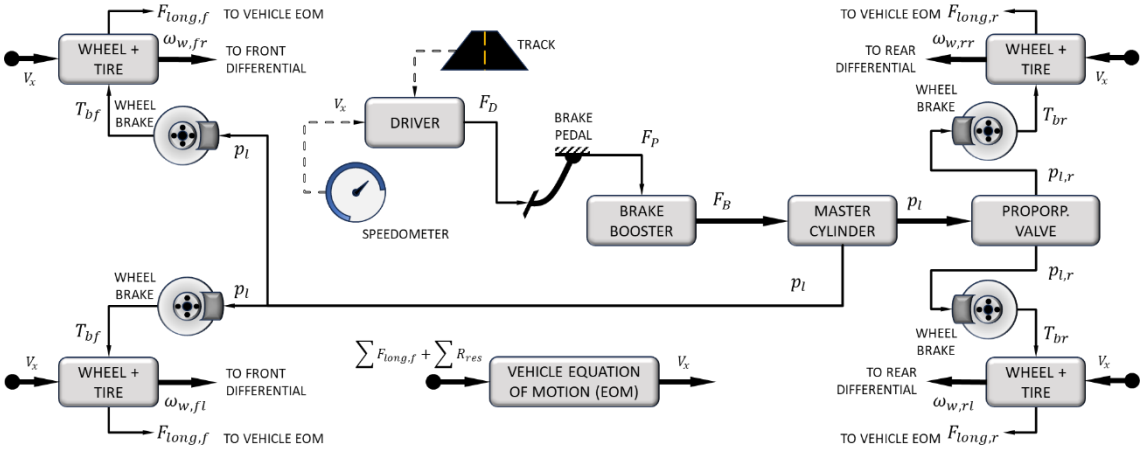

Figure 3. Hydraulic brake system block diagram (source: authors)

The vertical force, F_Z, that acts in each tire is calculated as a function of the static and dynamic transfer load (eq. 9).

$$F_{Z,f,j} = (1/2)(1 - \Psi + \chi a_g) \quad (9a)$$

$$F_{Z,r,j} = (1/2)(\Psi - \chi a_g) \quad (9b)$$

where,

$\Psi = a_1/L$

$\chi = h_{CG}/L$

$a_g = \dot{V}_x/g$

h_{CG} – height of vehicle center of gravity;

g – gravity.

When the brakes are applied, the vertical load on each wheel on the front axle increases, increasing tire grip. However, the load on the rear wheels decreases, reducing grip. In the model presented in this work, the brakes do not have ABS, but the block diagram structure allows it to include a control system acting in parallel. The braking force, F_D, is generated in the DRIVER block, at the chosen simulation time, then delivered to the BRAKE PEDAL block, by multiplying to F_P. The output BRAKE PEDAL force passes to the BRAKE BOOSTER block, where it is amplified to F_B. This force is passed to the MASTER CYLINDER block, converted into pressure (p_l) and then

distributed to the wheel brake lines. To minimize the risk of rear wheels premature locking, the braking system is equipped with a proportional valve (PROPROP. VALVE, Fig. 3), which reduces the pressure in the rear axle brake line to $p_{l,r}$, thus minimizing the dynamic weight transfer effect. In the WHEEL BRAKE blocks, the front/rear line pressures are converted to brake torque, T_{bf} and T_{br}. Each $T_{b,j}$ torque is then applied to the respective wheel, and is an input variable for each one's Euler equation of motion (eq. 6), within the WHEEL + TIRE block.

2.3 Tire models

Each tire model has an expression listed in Tab. 2 for calculating the longitudinal force (eq. 7). In all cases, there is dependence on the vertical load on the wheel, F_Z, and the longitudinal slip, i_x (eq 8).

Table 2. Tire models expressions

Tire model	Expression	Eq
Magic Formula [2]	$F_{long} = D\,\mathrm{sen}\{C\,\mathrm{tg}^{-1}\{B(i_x + S_h)(1-E) + E\,\mathrm{tg}^{-1}[B(i_x+S_h)]\}\} + S_v$	(10)
Burckhardt Model [7]	$F_{long} = sgn(i_x)\,[c_1(1-e^{-c_2 i_x}) - c_3 i_x]\,F_z$	(11)
Burckhardt Four Parameters Model [8]	$F_{long} = \{sgn(i_x)\,[c_1(1-e^{-c_2 i_x}) - c_3 i_x]\,e^{-c_4 v_x i_x}\}F_z$	(12)
Modified Burckhardt Model [4]	$F_{long} = sgn(i_x)\,[(1-e^{Q_1})\,\mu_{max} - c_3'\,(i_x)\,sgn(i_x) + c_4'\,i_x^2]\,F_z$ $Q_1 = -(c_1'/\mu_{max})(\lvert i_x\rvert + c_2'\,i_x^2)$	(13)
Dugoff Model(*) [9]	$F_{long} = C_x\,f_\lambda\,i_D/(1+i_D)$ $i_D = \begin{cases} -i_{long}/(1+i_x) & \text{(acceleration)},\quad i_x > 0 \\ -i_x \text{ (braking)}, & i_x < 0 \end{cases}$ $\lambda = F_z\left[\mu_{max}(1+i_D)/\left(2\sqrt{(C_x i_D)^2 + (C_\alpha \alpha)^2}\right)\right]$ $f_\lambda = \begin{cases} 1, & \lambda \geq 1 \\ (2-\lambda)\,\lambda, & \lambda < 1 \end{cases}$	(14)
Modified Dugoff Model(*) [10]	$F_{long} = G_x\,C_x\,f_\lambda\,i_D/(1+i_D)$ $G_x = (1{,}15 - 0{,}75\mu_{max})i_D^2 - (1{,}63 - 0{,}75\mu_{max})\,i_D + 1{,}27$	(15)
Pure Rolling Hypothesis	$\begin{cases} F_{long} = T_{wheel}/r_{din} \\ \omega_{w,j} = V_x/r_{din} \end{cases}$	(16a) (16b)

(*) i_D is called "Dugoff longitudinal slip", while the longitudinal slip is calculated by eq. 8.

The variables presented in eq. 10 to 15 (Tab. 2) are parameters specific to each mathematical tire model and depend on the surface's type. In eq. 16a, T_{wheel} is the torque applied to the wheel, originating from the differential or the brakes (one OR another). In this case, the wheel's equation of motion is neglected due to the kinematic restriction imposed in eq. 16b, where r_{din} is the tire dynamic radius. The variable μ_{max} is the peak coefficient between the tire and the pavement. Each one of the models was adapted to work with the longitudinal slip described in eq. 8, taking advantage of the general model's main characteristic, modularity.

The simulations are carried out by replacing the WHEEL + TIRE blocks and keeping the others unchanged. This model predicts the wheel locking under severe braking conditions. The vehicle's acceleration is calculated using Newton's equation written in a fixed frame of reference, as follows:

$$V_x = \int_{t=0}^{t=\tau}\left[\left(F_{long,f} + F_{long,r} - R_{aero} - R_{ramp}\right)/m_{body}\right]dt \tag{17}$$

where:

$$R_{aero} = \left(\rho_{air} A_f C_D V_x^2\right)/2 \tag{18}$$

$$R_{ramp} = m_{body} g \sin\phi \tag{19}$$

$$F_{long,j} = F_{long,j,jL} + F_{long,j,jR} \tag{20}$$

In the equations above ρ_{air} is the air density, C_D is the vehicle drag coefficient; A_f is the vehicle frontal area, and m_{body} is the vehicle mass.

3 Results and discussions

For each tire model listed in Table 2, 72 simulations were performed, combining four different types of surfaces (dry and wet asphalt, snow and icy road), four accelerator values (WOT, partial-70%, progressive-20%, and progressive-5%), and four different magnitude values of the force applied by the driver (P_F = 10, 50, 200, 400 N, eq. 21). The results were compared with analytical calculations based on Optimum Braking Conditions [6]. The simulations showed the divergences between the tire models and the theoretical condition. For dry asphalt the tire model that showed the least divergence was the Modified Burckhardt Model (eq. 13). Thus, this methodology highlighted the differences between the six tire models and the pure rolling condition.

$$F_D = P_F\sqrt{t_{sim} - t_{brake}} \tag{21}$$

The integration routine used in the simulations was ode15s, with a relative tolerance of 10^{-6} and a maximum integration step equal to 10^{-3} s. The initial speed $V_{x,0}$ of the vehicle was set as 5 km/h (minimum average value of a passenger vehicle moving in first gear with the engine at idle speed), and each wheel has an initial angular speed of $V_{x,0}/r_{din}$. It can be chosen whether the engine starts at wide-open throttle (WOT), partially opening the throttle, or at progressive load. The vehicle accelerates until reaching maximum speed, maintaining it until t_{brake} = 240 s, when the brake pedal is pressed according to eq. 21. Figure 4 shows the comparative graph of the longitudinal forces relevant to each model as a function of longitudinal slip. Figure 5 illustrates the angular speed of the front and rear wheels, and the vehicle's speed simulated with each tire model mentioned in Table 2. There is practically no variation in the maximum speed achieved, however during severe braking, for P_F = 400 N and from t = 240 s, the differences are noticeable – the front wheels lock prematurely. In the 4-parameter Burckhardt model (eq. 12), the front wheels lock before all others, while the rear wheels in the Dugoff model (eq. 14) lock in advance. It can be seen that the moment the front wheels brake, the rear wheels exhibit a behavior change, regaining speed shortly afterward. This is because the vehicle continues to move, but with the front wheels locked, then changing the dynamic weight transfer. This behavior does not exist in the pure rolling model, as there is no sliding.

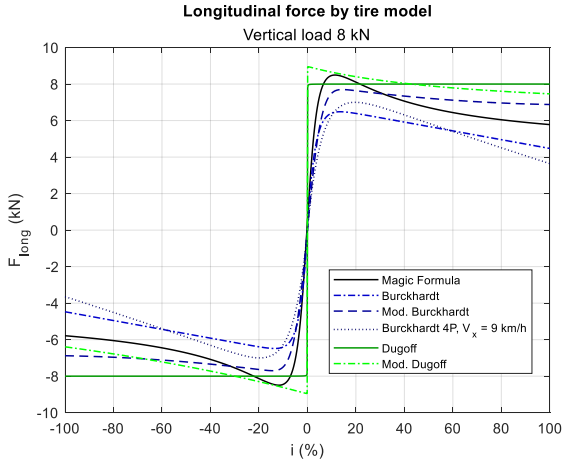

Figure 4 – Longitudinal force by tire model for vertical load F_z = 8 kN.

The vehicle exhibits a greater stopping distance when simulated with the 4-parameter Burckhardt model, while for the others the stopping difference is less than 2 seconds. The variation in the slope of the graphs is due to the locking of the front and rear wheels, and in this case, the model that presents the most differences is the 4-parameter Burckhardt model. The vehicle stops with all four wheels locked, except the pure rolling case. For all tire models, the tire-floor friction coefficient is considered the same, $\mu_{t\text{-}p}$ = 1.0 (dry concrete).

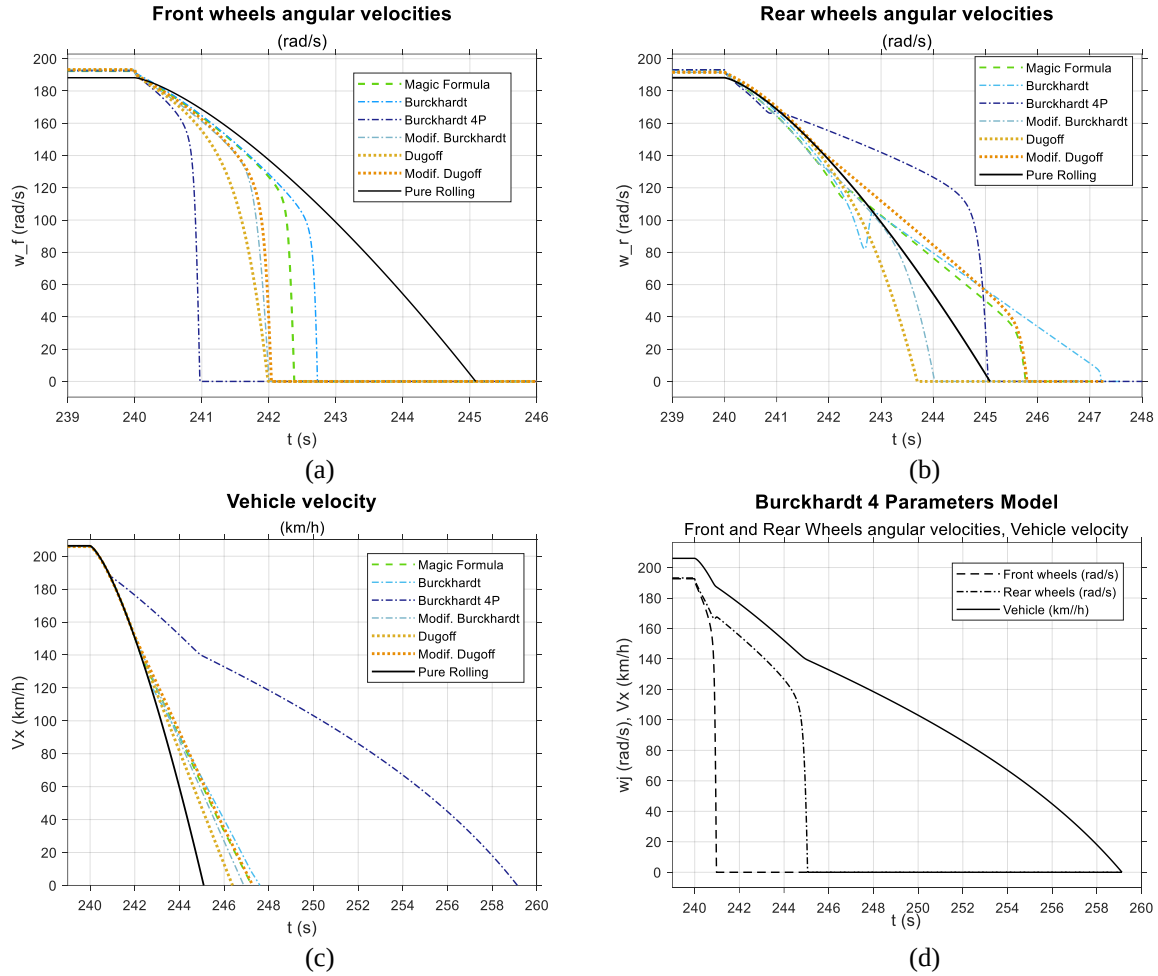

Figure 5 – Front (a) and rear (b) wheels behavior during braking; (c) vehicle velocity × time. (d) front and rear wheels and vehicle velocity behavior Burckhardt 4-parameters model.

Several tests with combinations of different surfaces (dry, wet asphalt, snow, and ice), accelerations, and traction were performed. The model that presented the best performance was the Modified Burckhardt method (eq. 13). Unfortunately, there is only one reference with this model and one set of parameters. As parameters for the Magic Formula are available for different surfaces, the Modified Burckhardt model was calibrated from synthetic measurements obtained with the Magic Formula model (eq. 10). For parameter estimation, the Levenberg-Marquardt method was applied using an iterative procedure following the hypothesis of additive errors, without bias and uncorrelated measurements [11]. The solution via inverse problems for the estimation was based on the objective function presented in Eq. (22), where **J** represents the Jacobian sensitivity matrix, λ_{lm} is a positive scalar called the damping parameter and **Ω** is the matrix with the diagonal terms of $[\mathbf{J}^T\mathbf{W}^{-1}\mathbf{J}]$. Both, λ_{lm} and **Ω** are responsible for damping the fluctuations and instabilities of the system. The vector of parameters **P** contains the constants c_1', c_2', c_3' and c_4' from Modified Burckhardt method, the synthetic measurements are represented by **Y** given by Magic Formula while the vector of estimations $\hat{\mathbf{Y}}$ are given by the Modified Burckhardt method.

$$\mathbf{P}^{k+1} = \mathbf{P}^k + \left[\, \mathbf{J}^T\, \mathbf{W}^{-1}\, \mathbf{J} + \lambda^{lm}\ \mathbf{\Omega}\, \right]^{-1} \mathbf{J}^T\, \mathbf{W}^{-1}\, [\mathbf{Y} - \hat{\mathbf{Y}}(\mathbf{P}^k)] \tag{22}$$

The longitudinal force F_x was obtained with the magic formula for each type of surface using the coefficients presented in Tab. 3. These synthetic measurements were inserted in the Levenberg-Marquardt algorithm that estimated the constants of the Modified Burckhardt method as indicated in Table 4.

Table 3. Magic Formula Coefficients

Surface	B	C	D	E	S_h
Dry asphalt	0.1187	1.65	5422.7	0.4045	0.1419
Wet asphalt	0.092	1.8	3187.5	-0.916	0.1419
Snow	0.0598	1.8	981.8	-0.916	0.1419
Ice	0.0598	1.8	490.9	-0.916	0.1419

Table 4. Estimates of Modified Burckhardt constants

Parameter	Dry asphalt (μ = 1.0)	Wet asphalt (μ = 0.65)	Snow (μ = 0.20)	Ice (μ = 0.15)
c_1'	20.9903	5.8543	1.2039	1.0958
c_2'	22.2684	20.4154	11.8157	1.6174
c_3'	0.1588	0.7451	0.1258	0.2246
c_4'	–0.1515	0.3555	0.136	0.1266

Using the parameters estimations, the longitudinal force F_x was obtained with the Modified Burckhardt method, and a comparison with the synthetic measurements is presented in Fig. 6 for different loads.

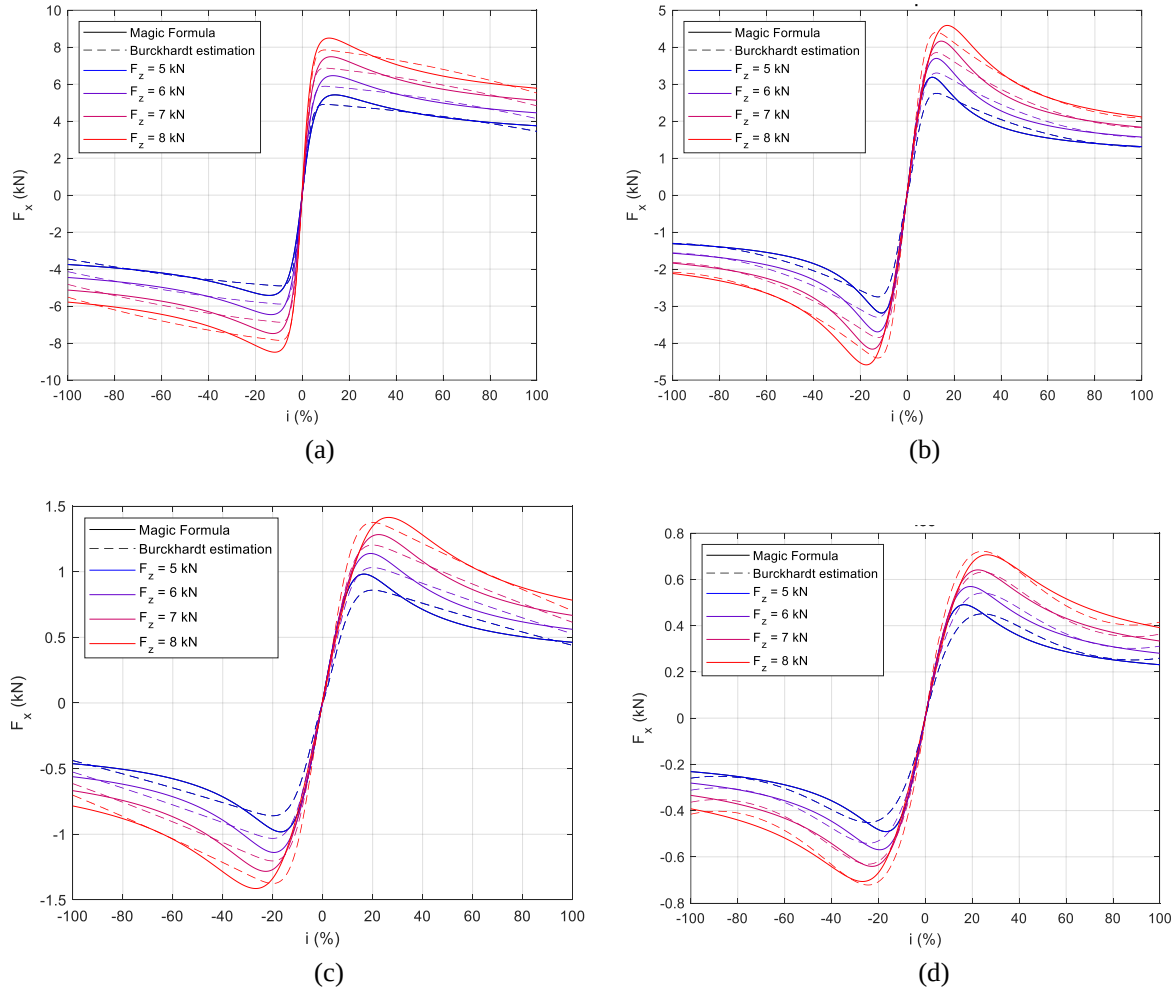

Figure 6 – Estimation and synthetic measurements for the longitudinal forces in different surfaces: (a) dry asphalt (b) wet asphalt; (c) snow (d) icy road.

4 Conclusions

In summary, the mathematical model modeled by Power Flow allows the replacement of blocks easily, given the inherent modularity. Maintaining causality, it is possible to replace blocks by others with different functions, and also incorporate control systems (e.g., TCS and ABS). However, it should be noted that such controllers were incorporated into existing systems, therefore the corresponding additional blocks must respect the original structure. It is even possible to simulate the vehicle's behavior with different tire models (e.g., Dugoff on the front axle and Magic Formula on the rear axle). The code of this model is also open, allowing the user to change the parameters according to their needs, increasing the degree of difficulty of some subsystems to bring the results closer to reality. The constitutive relations and expressions are found in the relevant literature. The Levenberg-Marquardt method was applied for parameter estimation allowing changes to mathematical models, reducing the need to search for parameters to represent tire behavior that depend on long and costly tests. Thus, the model presented in this work highlights the differences between at least six tire models, chosen because they are the most used in other articles in this area of knowledge, and how close they are to the theoretical calculation. It also shows how parameter estimation methods can be used to estimate the best parameters for the mathematical models of tire equations, which depend on field tests.

With this model structured in a block diagram and clearly modular, it was possible to find divergences between different mathematical models of tires, by simply replacing the corresponding blocks while maintaining the entire main structure and employing the Levenberg-Marquardt Method to obtain parameter values that represent the tire’s behavior on different surfaces.

Authorship statement. The authors hereby confirm that they are the sole liable persons responsible for the authorship of this work and that all material that has been herein included as part of the present paper is either the property (and authorship) of the authors or has the permission of the owners to be included here.

References

[1] C. Canudas-de-Wit, P. Tsiotras, E. Velenis, M. Basset, G. Gissinger, “Dynamic Friction Models for Road/Tire Longitudinal Interaction”, *Vehicle System Dynamics: International Journal of Vehicle Mechanics and Mobility*, 39:3, 189-226, 2003.
[2] Bakker, E., Pacejka, H., and Lidner, L., “A New Tire Model with an Application in Vehicle Dynamics Studies”, *SAE* Technical Paper 890087, 1989.
[3] R. T. Costa Neto, “Modelagem e Integração dos Mecanismos de Suspensão e Direção de Veículos Terrestres Através do Fluxo de Potência”, Doctoral thesis, PUC-Rio, 2008.
[4] X. Xia, L. Xiong, K. Sun, et al. “Estimation of maximum road friction coefficient based on Lyapunov method”, *Int.J Automot. Technol.* 17, 991–1002, 2016. (DOI: 10.1007/s12239-016-0097-7).
[5] R. N. Jazar, “Vehicle Dynamics, Theory and Applicantion”, Springer Science+Business Media, LLC, 2008.
[6] R. Limpert, “Brake Design and Safety”, 2nd ed., SAE, 1999.
[7] S. Savaresi, M. Tanelli, “Active Braking Control Systems Design for Vehicles”, Springer London Dordrecht Heidelberg New York, 2010.
[8] C. Elmas, U. Guvenc, M. U., Doğan, “Tire-Road Friction Coefficient Estimation and Experimental Setup Design of Electric Vehicle.”, *Balkan Journal of Electrical and Computer Engineering*, 3, 202-207, 2015. (DOI: 10.17694/bajece.8817)
[9] M. Belrzaeg, *et al*, “Vehicle dynamics and tire models: An overview”, *World Journal of Advanced Research and Reviews*, 12(01), 331–348, 2021.
[10] B. Lenzo, “Vehicle Dynamics - Fundamentals and Ultimate Trends”, *CISM International Centre for Mechanical Sciences*, 2022.
[11] H. R. B. Orlande, “Inverse Problems in Heat Transfer: New Trends on Solution Methodologies and Applications”, *Journal of Heat Transfer,* vol. 134, 031011-1–031011-13 2012.